Polymer Degradation and Stability 207 (2023) 110240

Contents lists available at ScienceDirect

Polymer Degradation and Stability

journal homepage: www.journals.elsevier.com/polymer-degradation-and-stability

Fire behaviour of EPDM/NBR panels with paraffin for thermal energy storage applications. Part 1: Fire behaviour

Francesco Valentini [a,*], Jean-Claude Roux [b], Josè-Marie Lopez-Cuesta [b,*], Luca Fambri [a], Andrea Dorigato [a], Alessandro Pegoretti [a,*]

[a] Department of Industrial Engineering and INSTM Research Unit, University of Trento, Via Sommarive 9, 38123 Trento, Italy
[b] Polymer Composites Hybrids (PCH) – IMT Mines Alès, 6 avenue de Clavières, 30319 Alès Cedex, France

ARTICLE INFO

Keywords:
EPDM
NBR
Phase change materials
Fire behaviour
Flame retardancy
Cone calorimetry

ABSTRACT

In this work the fire behaviour of elastomeric panels made of an Ethylene-Propylene Diene Monomer (EPDM) rubber filled with a shape-stabilized paraffin with a melting point of 28 °C and covered with a nitrile-butadiene rubber (NBR) envelope, developed for thermal energy storage applications, was investigated for the first time. The panels were prepared using four different flame retardants (FR) and in order to test their efficacy they were dispersed selectively only in the core material, or in the envelope or in both of them. Cone calorimeter and epiradiateur tests pointed out the efficacy of the clay used for the shape stabilization of paraffin and of the external NBR envelope. Moreover, it was possible to demonstrate that a flame retardant based on ammonium polyphosphate and aluminium diethyl phosphinate could achieve the best fire performances. It was also verified that the combination of the FR both in the core and in the envelope led to the best results thanks to the physico-chemical and chemical interactions between clay, talc, kaolin and silicon with ammonium polyphosphate. The best composition allowed to decrease the peak of the heat release rate (HRR) from 318 kW/m^2 to 209 kW/m^2 and the MARHE (parameter describing the intensity of the combustion over the whole process of thermal degradation) from 239 kW/m^2 to 175 kW/m^2. Moreover, regarding the ability to self-extinguish, the number of ignitions at epiradiateur test was increased from 4 to 8 within 5 min and the total combustion time from 391 to 288 s. The improvement of the fire behaviour of EPDM/NBR panels with paraffin makes possible future applications in the field of thermal energy storage of buildings.

1. Introduction

Nowadays, due to global warming and climate change, it is essential to find an equilibrium between energy demand and energy resources [1]. Solar energy is the largest energy source on Earth and the energy that Earth receives from the sun is around 10,000 higher than the total energy demand. Among different technologies used to convert solar energy into other energy sources, heat storage consists in the collection of solar energy to obtain and store heat without further transformations [2–8]. Thermal energy storage (TES) is usually based on the phase transition of so-called Phase Change Materials (PCMs), that occurs at constant temperature and provides high energy storage capability [6, 9-12]. Paraffins are the most used PCMs thanks to the high heat of fusion and low price; in literature, several applications of paraffin for the thermal energy storage of buildings are reported [13–16]. One problem of using phase change materials is their leakage in the molten state which requires their encapsulation and/or shape stabilization within polymer matrices [17–28] or ceramic structures [29]. The second and main problem related to the possible use of PCMs in building application is their flammability and the fact that in case of fire they represent additional fuel. Different methods to reduce the flammability of materials containing PCMs have been reported in the literature: the first one consists in the encapsulation of the composite building block within two layers of non-combustible concrete; the second one involves the shape stabilization of the PCM within a polymeric material combined with the use of flame retardants [30–32]. Three main categories of flame retardants can be identified on the market. The first one is represented by halogenated compounds (such as chlorinated paraffins) known as flame quencher, due to their ability to extinguish nearby the flame [31,33-35]. Nevertheless, their use is decreasing for many applications due to

* Corresponding authors.
E-mail addresses: francesco.valentini@unitn.it (F. Valentini), jose-marie.lopez-cuesta@mines-ales.fr (J.-M. Lopez-Cuesta), alessandro.pegoretti@unitn.it (A. Pegoretti).

https://doi.org/10.1016/j.polymdegradstab.2022.110240
Received 3 October 2022; Received in revised form 16 December 2022; Accepted 21 December 2022
Available online 22 December 2022

environmental concerns [36]. The second category comprises materials that by increasing the temperature decompose endothermically, subtracting heat from the flame; examples are magnesium hydroxide and aluminium trihydroxide [31,34]. The third category is that of intumescent flame retardants, that when heated beyond a critical temperature form an intumescent layer able to protect the underlying material from excessive temperature increase, oxygen diffusion and exposure to the ignition source. The formation of the intumescent layer is possible thanks to the combination of a charring and foaming mechanism: a precursor of carbonization catalyst such as ammonium polyphosphate (APP) is usually combined with a carbonization agent such as pentaerythritol (PER) or polymers able to char intrinsically and with a blowing agent such as melamine polyphosphate (MPP) [37–41]. Another category of compounds involved in fire retardancy comprises synergistic agents: they are materials that, combined with a particular FR, improve its flame retardancy making the global effect of the two components greater than the sum of the two individual effects. Examples are antimony oxide with halogenated flame retardants [42] or montmorillonite and talc with hydrated minerals [43–45], or montmorillonite and talc with ammonium polyphosphate [34,38,46-48]. The synergistic effect of montmorillonite consists in the formation of a carbonaceous-silicate charred layer that protects the underlying material from excessive temperature increase. It is usually combined with intumescent fire retardants and heat absorbers [34,46,47,49]. The synergistic effect of talc was reported by Almeras et al. [50] and Dzulkafli et al. [51] that verified the improvement of the intumescent effect of ammonium polyphosphate thanks to the formation, on the char, of a silicate layer protecting the underlying material. Thuechart et al. [52] verified the synergistic effect of kaolin with intumescent flame retardants (ammonium polyphosphate + pentaerythritol + melamine). In particular, Ullah et al. [53] found that the synergistic effect of kaolin led to an enhanced char expansion on the sample surface with a consequent improved heat shielding effect of the substrate. Some authors also reported the synergistic effect of silica on intumescent flame retardants: in particular SiO_2 promoted the esterification reaction responsible of the formation of the carbon layer in intumescent flame retardants [54,55]. Zinc borate is another flame retardant with multiple working principles: by temperature increase it dehydrates endothermically subtracting heat to the flame, at a certain temperature the formation of B_2O_3 contributes to the formation of a dense char layer protecting the underlying material from the flame and restricting the generation of combustible gases and oxidation reactions [56–58]. Chen et al. [57] reported the synergistic effect of zinc borate with intumescent flame retardants (pentaerythritol + melamine phosphate) added to the composition of EPDM/polypropylene composites. Sittisart et al. [31] investigating the addition of FRs on the fire behaviour of RT21HC paraffin shape-stabilized within an HDPE matrix, observed that the best performances were obtained combining 10 wt% of APP with 10 wt% of PER and 5 wt% of montmorillonite or combining 10 wt% of APP with 10 wt% of expanded graphite. Cai et al. [47] investigating the efficacy of different FRs on the fire behaviour of a paraffin with a melting point of 56 °C and shape-stabilized within an HDPE matrix, obtained the best results combining 15 wt% of MPP with 10 wt% of PER.

Considering the possible application of EPDM/NBR/paraffin panels for building applications, the risks associated to the use of such materials in case of fire and the lack of studies on the fire behaviour of similar systems, this work investigates the effect of four commercial flame retardants on the fire properties of the prepared panels, previously characterized [16]. Based on the bibliographic review and on the possible positive interactions between the components of the investigated systems and relevant available flame retardants, four FR were selected: two based on ammonium polyphosphate, one on organic phosphinate and one on zinc borate. Cone calorimeter tests and tests to evaluate the self-extinguishing ability of such materials were carried out.

2 Experimental part

2.1. Materials

Vistalon® 2504 EPDM rubber is an amorphous terpolymer with a broad molecular weight distribution, a low Mooney viscosity (ML 1+4, 125 °C) of 25 MU, a medium diene content (4.7 wt% of ethylidene norbornene), a low ethylene content (58 wt%), and was purchased from Exxon mobil (Irving, TX, USA). EPDM rubber is characterized by excellent resistance to UV and ozone because EPDM is constituted by a fully saturated polymer backbone [59], with some residues of pendant unsaturated groups. Rubitherm RT28HC paraffinic wax, with a melting point of 28 °C and a specific melting enthalpy (ΔH_m) of around 250 J/g was purchased from Rubitherm GmbH (Berlin, Germany). Zinc oxide (curing activator), stearic acid (curing activator and lubricating agent) and sulphur (vulcanizing agent) were supplied by Rhein Chemie (Cologne, Germany). The accelerators tetramethylthiuram disulphide (TMTD) and zinc dibutyl dithiocarbamate (ZDBC) were obtained from Vibiplast srl (Castano Primo (MI), Italy). Carbon black N550 obtained from Omsk Carbon group (Omsk, Russia) was used as a reinforcing filler. The elastomeric compound used for the preparation of the samples consisted of 100 phr of Vistalon® 2504, 3 phr of sulphur, 3 phr of zinc oxide, 1 phr of stearic acid, 20 phr of carbon black, 0.87 phr of TMTD and 2.5 phr of ZDBC. Organomodified clay Cloisite® 20 was obtained from BYK-Chemie GmbH (Wesel, Germany). Cloisite®20 is a bentonite or montmorillonite modified with bis(hydrogenated tallow alkyl) dimethyl ammonium chloride and according to the datasheet, it is characterized by a density of 1.8 g/cm^3, by a particle size lower than 10 μm and by a lamellar spacing of 3.2 nm [60–62].

Exolit® AP766 (AP766), a non-halogenated flame retardant (phosphorus content around 23 wt%, nitrogen content around 14 wt%), was provided by Clariant GmbH (Ahrensburg, Germany). As reported in the Part 2 of this work [63], this FR contained ammonium polyphosphate and aluminium diethyl phosphinate as synergistic agent. Exolit® AP423 (AP423), a non-halogenated flame retardant consisting of ammonium polyphosphate (phosphorus content around 31 wt%), was provided by Clariant GmbH (Ahrensburg, Germany). Exolit® OP950 (OP950), a non-halogenated flame retardant containing zinc diethyl phosphinate (phosphorus content around 23 wt%), was provided by Clariant GmbH (Ahrensburg, Germany). Zinc borate Firebrake® ZB (ZB), chemical formula $2ZnO{\cdot}3B_2O_3{\cdot}3.5H_2O$, was provided by Borax (Boron, USA). It was characterized by a content of boric oxide of 48 wt%, zinc oxide of 37.4 wt%, and water of 14.5 wt%.

NBR (nitrile-butadiene rubber) foils (thickness equal to 0.4 mm), with high acrylonitrile content (45 wt%), without FR (used as reference) were purchased on the market. The NBR foils contained around 33 wt% of inorganic fillers in their composition (i.e. talc (11 wt%), kaolin (11 wt %) and silica (11 wt%)). Talc Mistron® R10 C and kaolin ARGIREC^{TM} B24 were provided by Imerys Talc (Paris, France) and were used to increase the barrier effect of NBR rubber against gases and oils. Silica ULTRASIL VN 3 was provided by Evonik AG (Essen, Germany) and was used to create a physical crosslinking effect and to control the rheology. Further NBR foils were prepared by calendering adding a certain amount of the four FRs (18 wt%) to the neat NBR foils purchased on the market.

2.2. Samples preparation

In order to modify the rheology of the system and to maximize the quantity of paraffin that could be mixed with the rubber matrix, liquid paraffin wax was firstly mixed with Cloisite® 20 clay (at a constant paraffin/clay ratio of 3:1 [64]) and ultrasonicated for 5 min at 30 °C using a Hielscher UP400S device (Teltow, Germany), equipped with a cylindrical sonotrode with a diameter of 15 mm and operating at a power of 400 W.

All the samples were prepared by melt compounding in an internal mixer (Thermo Haake Rheomix® 600), operating at a temperature of

40 °C and at a rotating speed of 50 rpm. First, the EPDM sample was prepared according to the composition reported in Table 1: the elastomer was fed into the mixer with the carbon black and mixed for 5 min, then sulphur, zinc oxide, stearic acid and the accelerators were added and mixed for other 5 min. Then the procedure was different for samples with or without phase change material (PCM) and with or without flame retardants (FR), as follows:

- To produce the sample with PCM, after a mixing time of 10 min, the PCM-clay mixture was added to the mixer and mixed for 30 min, reaching a mixing time of 40 min [16].
- To produce samples with PCM and with FR, after the addition of the PCM-clay mixture and the mixing for 30 min, FR were gradually added and mixed for further 10 min, reaching a total mixing time of 50 min.
- To produce samples without PCM and with FR, after the preparation of the EPDM compound, FR were gradually added and mixed for further 10 min, reaching a total mixing time of 20 min.

The compounds were then directly vulcanized in case they did not contain PCM, or previously covered with a NBR envelope, in the other cases:

- To produce the EPDM reference sample and samples without envelope, the material was vulcanized at a temperature of 170 °C for 20 min, under a Carver hot press at a pressure of 8 bar, obtaining square sheets with dimensions 110×110×5 mm^3 and 70×70×5 mm^3.
- To produce samples with envelope, the compound was transferred in a mould covered with a 0.4 mm layer of NBR rubber (ENV) used in order to avoid paraffin leakage. The vulcanization process of the resulting compound was carried out under a Carver hot press at a pressure of 2 bar, for 20 min at a temperature of 170 °C. In this way, square sheets with dimensions of around 110×110×5 mm^3 and 70×70×5 mm^3 were obtained.

In Table 1 the main properties of the selected FR are reported, while the list of the prepared samples along with their codes is shown in Table 2 (see also Table S1 for more details). The amount of paraffin RT28HC and of FR in the core reported in Table 2 (wt%, phr) were calculated with respect to the total mass of the EPDM/paraffin/clay compound (E+P) and not considering the mass of the NBR envelope (ENV). In Fig. 1a a picture of the E+P+ENV sample is shown, while a scheme of the vulcanization process is shown in Fig. 1b.

For simplicity it is possible to divide the prepared samples into 6 categories:

- Reference samples with and without PCM (with and without clay), with and without ENV.
- E+P+FR: samples with PCM, without ENV and with FR in the core.
- ENV+FR: envelopes with FR.
- E+P+FR+ENV: samples with PCM, with ENV and with FR only in the core.
- E+P+ENV+FR: samples with PCM, with ENV and with FR only in the ENV.
- E+P+FR+ENV+FR: samples with PCM, with ENV and with FR in the core and in the ENV.

Table 1
Main properties of the FRs used in the work [65–68].

Material	P [wt%]	N [wt%]	Density [g/cm^3]	Decomposition temperature [°C]
AP766	23.0–25.0	14.1–16.4	1.6	> 240
AP423	31.0–32.0	14.0–15.0	1.9	> 275
OP950	19.5–20.5	-	1.3	> 350
ZB	-	-	2.8	> 290

Table 2
Composition, code and estimated TES performance of the prepared samples.

Sample code	RT28HC* [wt% - phr]	FR	FR in core [wt% - phr]	FR in ENV [wt% - phr]	TES** [J/g]
E	-	-	0	-	-
E+P	56.8–263	-	0	-	125
E+P_NC***	56.8–171	-	0	-	125
E+P+ENV	56.8–263	-	0	0	97
E+P_NC***+ENV	56.8–171	-	0	0	97
E+P+766	45.5–263	AP766	20–115	-	100
E+P+423	45.5–263	AP423	20–115	-	100
E+P+950	45.5–263	OP950	20–115	-	100
E+P+ZB	45.5–263	ZB	20–115	-	100
ENV	-	-	-	0	-
ENV+766	-	AP766	-	18–40	-
ENV+423	-	AP423	-	18–40	-
ENV+950	-	OP950	-	18–40	-
ENV+ZB	-	ZB	-	18–40	-
E+P+766+ENV	45.5–263	AP766	20–115	0	78
E+P+423+ENV	45.5–263	AP423	20–115	0	78
E+P+950+ENV	45.5–263	OP950	20–115	0	78
E+P+ZB+ENV	45.5–263	ZB	20–115	0	78
E+P+ENV+766	56.8–263	AP766	0	18–40	97
E+P+ENV+423	56.8–263	AP423	0	18–40	97
E+P+ENV+950	56.8–263	OP950	0	18–40	97
E+P+ENV+ZB	56.8–263	ZB	0	18–40	97
E+P+766+ENV+766	45.5–263	AP766	20–115	18–40	78
E+P+423+ENV+423	45.5–263	AP423	20–115	18–40	78
E+P+950+ENV+950	45.5–263	OP950	20–115	18–40	78
E+P+ZB+ENV+ZB	45.5–263	ZB	20–115	18–40	78

* Values evaluated with respect to the total mass of the core material (not considering the envelope).
**Estimated thermal energy storage (TES) values (i.e. melting enthalpy) evaluated on the basis of the results reported in [16].
***Samples prepared without the addition of clay.
Acronyms: E=EPDM, P=paraffin Rubitherm® RT28HC, ENV=NBR envelope, 766=Exolit® AP766, 423=Exolit® AP423, 950=Exolit® OP950, ZB=Firebrake® ZB

2.3. Experimental methodologies

2.3.1. Scanning electron microscopy

Samples before combustion were observed using a Jeol IT300 scanning electron microscope; before the observations of the cryofractured surfaces, the specimens were metalized under vacuum through the deposition of a thin electrically conductive Pt/Pd coating. Only selected compositions have been observed: E+P+ENV, E+P+766+ENV+766, E+P+423+ENV+423.

2.3.2. Fire tests

Cone calorimeter tests were carried out using a Fire Testing Technology cone calorimeter according to ISO 5660 standard. Two specimens, instead of three, were tested for each sample due to material constraints. The specimens, with dimensions of 110×110×5 mm^3 were placed in a standard sample holder used in order to expose a surface of 88.4 cm^2 to the heat flow (please note that despite the larger size of the specimens, the exposed surface is the same of regular specimens). The cone temperature was set a 642 °C in order to obtain a heat flux of 35 kW/m^2 at a distance of 25 mm. The exhaust gas flow was set to 24 l/s. The ignition time (t_{ign}), the flameout time (t_{Fout}), the first peak of the heat release rate (HRR_{peak1}) and the related time (t_{HRR1}), the first peak of the heat release rate (HRR_{peak2}) and the related time (t_{HRR2}), the residual mass (m_{res}) and the maximum average rate of heat emission (MARHE) were evaluated. The ARHE (average rate of heat emission) was calculated according to Eq. 1 [69]:

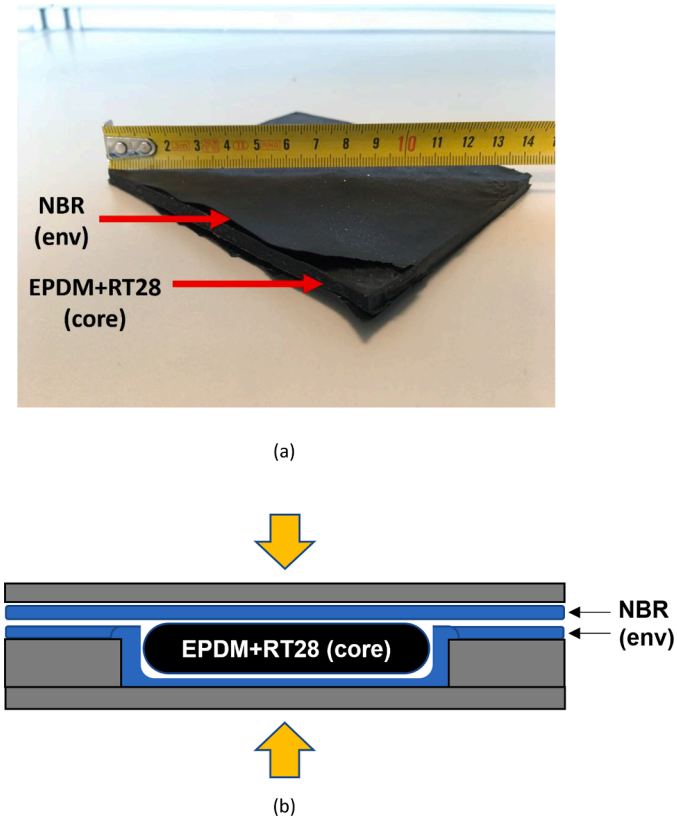

Fig. 1. (a) Representative picture of E+P+ENV sample (the specimen was cut in order to show the core material); (b) schematic representation of the vulcanization process through hot pressing (the grey structure represents the mould used to prepare the squared specimens under the hot-plate press).

$$ARHE(t_n) = \frac{\sum_2^n \left((t_n - t_{n-1}) * \frac{q_n + q_{n-1}}{2}\right)}{t_n - t_0} \quad (1)$$

t_n: time, q_n: rate of heat released at t_n

The self-extinguishing ability of the produced samples was studied using a radiant heat source (epiradiateur AFNOR NF P92-505). The test was carried out on specimens with dimensions of 70×70×5 mm^3, placed on a metallic grid and exposed to a heat source of 500 W, at a distance of 30 mm (irradiance of 35 kW/m^2). The heat source was removed after 5 s from each ignition and replaced after the flame extinction. The ignition time (t_{ign}), the number of ignitions over five minutes (N_{ign}), the mean time of combustion between to ignitions ($t_{combustion\text{-}2ign}$) and the total combustion time (t_{tot}) were evaluated. Moreover, during the test the surface temperature of the samples, on the opposite side with respect to the flame, was monitored using a pyrometer and the temperature as function of time as well as the maximum temperature (T_{max}) were reported. Two specimens were tested for each sample. Epiradiateur tests were performed instead of UL94 tests because they provide more information, particularly useful especially in case of complex systems.

2.3.3. Thermogravimetric analysis

Thermogravimetric analysis (TGA) was performed using a Mettler TG50 thermobalance under an air-flow of 100 ml/min in a temperature range between 30 and 700 °C, at a heating rate of 10 °C/min. Alumina crucible without cup containing around 40 mg of material were used. The temperature associated to a mass loss of 5% ($T_{5\%}$) and the temperatures associated to the maximum degradation rate of the constituents (T_{peak1}, T_{peak2}, T_{peak3}) and the residual mass at 700 °C (m_{700}) were determined.

3. Results and discussion

3.1. Scanning electron microscopy (SEM)

Looking at the SEM pictures of sample E+P+ENV before combustion, shown in Fig. 2 (a, b), it is possible to observe the similarity with SEM pictures of the same composition reported in a previous work [70]: the presence of small holes can be observed, the morphology is uniform and the presence of impurities or contaminants cannot be detected. From SEM pictures of sample E+P+766+ENV+766 at 100x shown in Fig. 2c, it is possible to observe the presence of particles with dimensions of around 15 μm that can be ascribed to some components of the FR. At higher magnification (1000x, Fig. 2d), the presence of few particles with dimensions of around 1–1.5 μm can be detected. Observing the SEM pictures of sample E+P+423+ENV+423 at 100x shown in Fig. 2e, it is possible to notice that the microstructure is similar to that of sample E+P+766+ENV+766 shown in Fig. 2c with the difference that in this case no particle can be detected. On the other hand, at higher magnification (Fig. 2f) the presence of several small particles with dimension of around 1–2 μm can be detected. Considering that FR AP423 consists of neat ammonium polyphosphate, it is possible to hypothesise that these particles consist of APP (the same also for the few particles observed in Fig. 2d). Conversely, the particles with higher dimension observe in Fig. 2c, are probably related to the synergistic agents present in the FR AP766.

3.2. Cone calorimeter tests

Looking at the curves obtained from cone calorimeter tests and representing the heat release rate (HRR) as function of time, shown in Fig. 3 (a-f), it is possible to verify the effect of the flame retardants (FRs) applied in different ways to the prepared samples and to compare the fire behaviour with respect to the reference samples without FR (Fig. 3a).

3.2.1. Reference samples

From Fig. 3a it is possible to compare the curves of the reference samples without FR. The EPDM sample is characterized by a long ignition time and by a single HRR peak. The addition of PCM (sample E+P) leads to a very rapid ignition and to a more violent combustion with HRR values higher than 450 kW/m^2. It is very interesting to observe the behaviour of the E+P-NC sample, prepared with the same composition of the E+P but without clay: the combustion is very violent with the HRR that reaches values up to 650 kW/m^2. A similar behaviour can be observed comparing the curves of the E+P+ENV with the E+P+ENV_NC: the latter is characterized by a first HRR peak with the same intensity but by a second HRR peak with much higher intensity. These behaviours confirm the beneficial effect of the clay that is probably related to the formation of a carbonaceous-silicate charred barrier layer that protects the underlying material [49]. This effect can be also quantified looking at the data listed in Table 3: a strong decrease of HRR_{peak2} from 618 kW/m^2 in case of E+P_NC to 467 kW/m^2 in case of E+P and of MARHE from 479 kW/m^2 to 383 kW/m^2 can be observed. Moreover, the t_{Fout} is increased from 653 s to 920 s. Comparing the curves E+P and E+P+ENV, it is immediately clear the beneficial effect of the envelope: the E+P+ENV sample is characterized by lower HRR values and longer combustion times (both factors are indicating the lower violence of the combustion). Despite the absence of flame retardants, it is possible to hypothesise a positive effect of the mineral fillers present in the envelope (talc, kaolin and silica) in the formation of a protective layer against flame propagation [71,72]. Moreover, it can be also considered that NBR rubber is less flammable with respect to EPDM [73], and that in the sample E+P+ENV the paraffin is more diluted in the whole material.

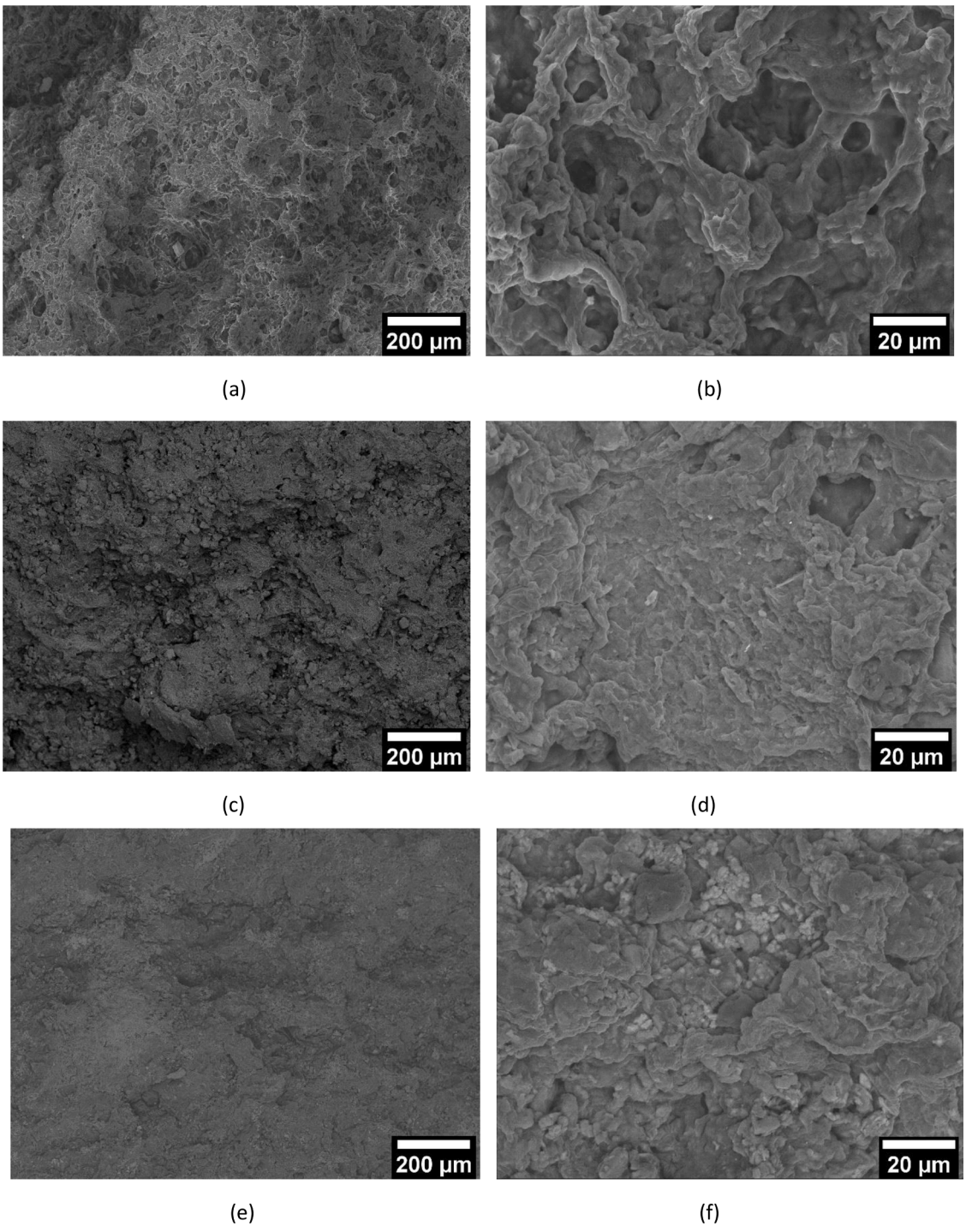

Fig. 2. SEM pictures in BSE mode of selected compositions before fire tests at 100x (a, c, e) and 1000x (b, d, f): E+P+ENV (a, b), E+P+766+ENV+766 (c, d) and E+P+423+ENV+423 (e, f).

3.2.2. *Samples without envelope and with FRs in the core*

From Fig. 3b it is possible to observe that in case of samples with FRs but without envelope the HRR curves are characterized by two peaks, the first probably caused by the combustion of paraffin present on the samples' surfaces and the second due to the combustion of the EPDM matrix. It is also possible to observe that all the FRs lead to a decrease of HRR values. In particular, looking at the results reported in Table 3, it is possible to observe that the best result is obtained using the AP766: the HRR_{peak1} and HRR_{peak2} are decreased from 412 kW/m^2 and 467 kW/m^2 (in case of E+P) down to 331 kW/m^2 and 315 kW/m^2, respectively in case of E+P+766. The MARHE is decreased from 383 kW/m^2 to 276 kW/m^2. E+P+423 composition gives interesting results but lower performances in comparison with E+P+766. ZB seems to have a beneficial effect only on the t_{ign} (17 s) probably due to the lack of interaction with the clay. Similarly, also the OP950 shows limited benefits of the flame retardancy of the material.

3.2.3. *Envelopes*

From Fig. 3c it is possible to observe that in case of envelopes the combustion is violent and very rapid due to the low amount of material (the envelopes were 0.4 mm thick instead of 5 mm of other samples). Also in this case all the FRs lead to an improvement of the fire behaviour

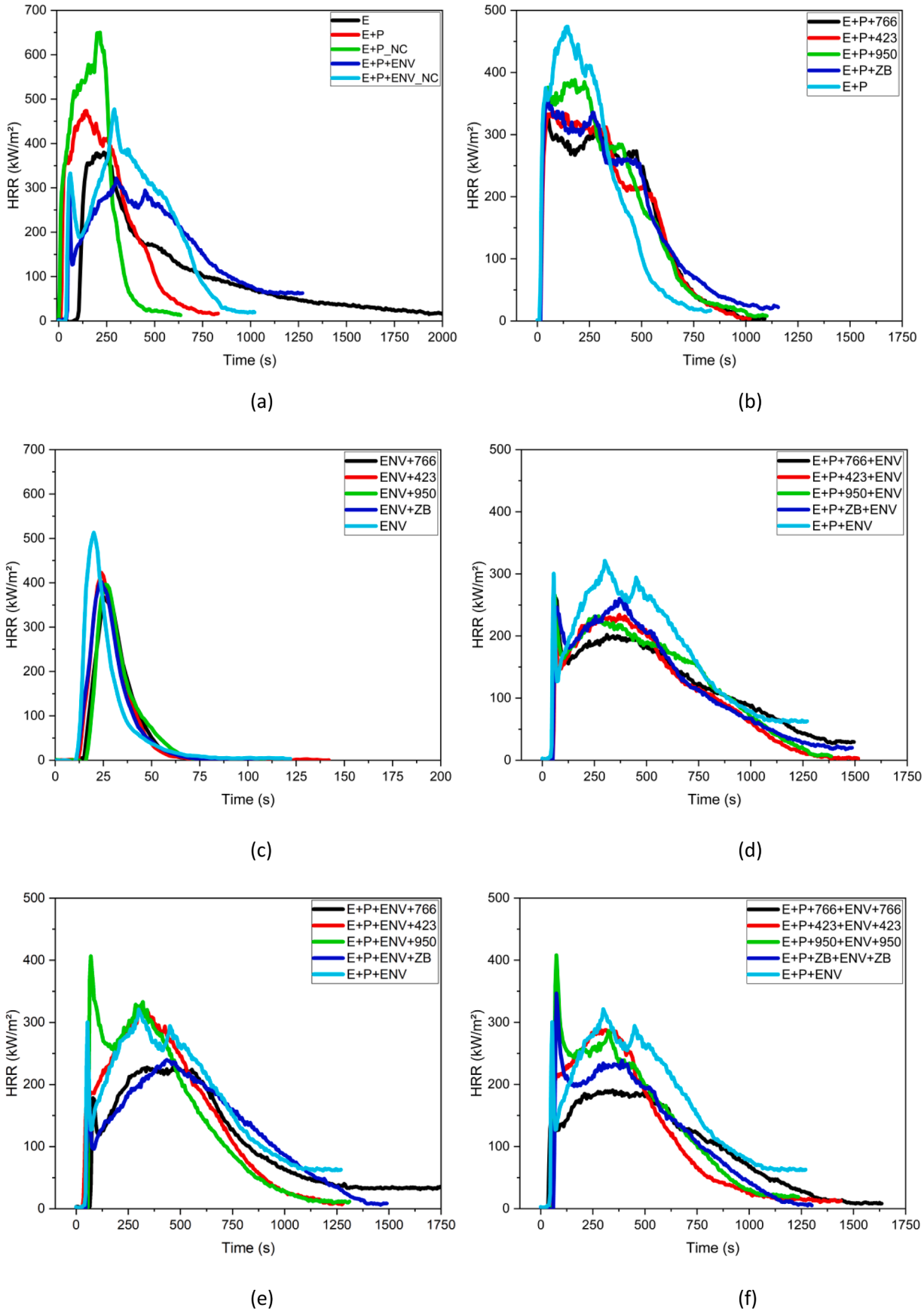

Fig. 3. Representative curves of HRR as function of time for the prepared samples: reference samples (a), E+P+FR (b), ENV+FR (c), E+P+FR+ENV (d), E+P+ENV+FR (e), E+P+FR+ENV+FR (f).

Table 3
Results of cone calorimeter tests.

Sample	t_{ign} [s]	t_{Fout} [s]	t_{HRR_peak1} [s]	HRR_{peak1} [kW/m^2]	t_{HRR_peak2} [s]	HRR_{peak2} [kW/m^2]	MARHE [kW/m^2]	m_{res} [%]
E	97 ± 11	1732 ± 243	-	-	220 ± 21	397 ± 24	223 ± 1	17.0 ± 1.3
E+P	18 ± 5	920 ± 127	-	-	147 ± 3	467 ± 9	383 ± 8	17.0 ± 0.1
E+P_NC	12 ± 9	653 ± 25	-	-	192 ± 32	618 ± 46	479 ± 32	4.5 ± 1.0
E+P+ENV	42 ± 5	1343 ± 103	52 ± 3	266 ± 49	315 ± 21	318 ± 4	239 ± 9	31.3 ± 0.5
E+P+ENV_NC	48 ± 11	915 ± 148	62 ± 3	348 ± 22	247 ± 60	425 ± 74	273 ± 29	24.5 ± 5.5
E+P+766	15 ± 1	1088 ± 4	45 ± 0	331 ± 1	225 ± 255	315 ± 25	276 ± 3	24.8 ± 0.8
E+P+423	20 ± 3	1100 ± 113	67 ± 25	335 ± 1	227 ± 201	334 ± 3	292 ± 3	29.3 ± 0.2
E+P+950	13 ± 2	1050 ± 71	45 ± 7	375 ± 1	195 ± 21	401 ± 18	345 ± 10	23.8 ± 2.1
E+P+ZB	17 ± 1	1103 ± 74	47 ± 3.5	351 ± 11	167 ± 166	356 ± 5	301 ± 4	29.7 ± 0.3
ENV	10 ± 0	145 ± 32	20 ± 0	512 ± 1	-	-	207 ± 3	57.9 ± 4.0
ENV+766	14 ± 3	118 ± 11	25 ± 0	358 ± 14	-	-	150 ± 1	60.8 ± 0.9
ENV+423	15 ± 4	125 ± 24	25 ± 2	391 ± 44	-	-	162 ± 23	62.3 ± 3.9
ENV+950	14 ± 3	104 ± 6	25 ± 1	402 ± 8	-	-	159 ± 16	76.9 ± 18.8
ENV+ZB	10 ± 1	106 ± 1	23 ± 1	410 ± 11	-	-	179 ± 3	64.4 ± 0.7
E+P+766+ENV	43 ± 6	1253 ± 342	65 ± 1	301 ± 57	285 ± 35	259 ± 80	209 ± 56	40.8 ± 2.6
E+P+423+ENV	50 ± 8	1321 ± 274	60 ± 7	225 ± 14	327 ± 60	246 ± 17	188 ± 4	43.2 ± 4.1
E+P+950+ENV	43 ± 6	1161 ± 317	60 ± 1	299 ± 47	260 ± 14	272 ± 56	214 ± 40	37.1 ± 3.2
E+P+ZB+ENV	53 ± 1	1390 ± 134	67 ± 3	251 ± 7	377 ± 11	266 ± 8	203 ± 6	38.8 ± 4.3
E+P+ENV+766	82 ± 18	1672 ± 279	95 ± 21	213 ± 49	357 ± 25	250 ± 32	188 ± 15	35.9 ± 0.2
E+P+ENV+423	46 ± 16	1295 ± 21	65 ± 21	202 ± 41	297 ± 39	341 ± 28	244 ± 4	33.8 ± 0.6
E+P+ENV+950	67 ± 14	1318 ± 11	80 ± 14	422 ± 22	327 ± 11	331 ± 3	250 ± 9	34.8 ± 0.6
E+P+ENV+ZB	67 ± 27	1388 ± 145	80 ± 28	272 ± 108	412 ± 32	280 ± 56	206 ± 41	35.4 ± 0.8
E+P+766+ENV+766	46 ± 11	1390 ± 346	190 ± 198	186 ± 58	337 ± 11	209 ± 26	175 ± 20	33.1 ± 12.5
E+P+423+ENV+423	128 ± 116	1315 ± 177	145 ± 113	309 ± 136	375 ± 141	335 ± 64	213 ± 20	33.3 ± 12.9
E+P+950+ENV+950	57 ± 7	1373 ± 194	70 ± 7	352 ± 78	340 ± 21	263 ± 33	212 ± 16	41.4 ± 0.4
E+P+ZB+ENV+ZB	90 ± 38	1270 ± 42	102 ± 39	407 ± 86	387 ± 3	259 ± 29	199 ± 9	45.4 ± 1.0

with a decrease of the HRR values. In particular, looking at the results reported in Table 3, it is possible to observe that the best result is also obtained using the AP766: the HRR_{peak1} is decreased from 512 kW/m^2 of ENV down to 352 kW/m^2, respectively. The MARHE is decreased from 207 kW/m^2 to 150 kW/m^2. The t_{ign} is maximized using AP723 (20 s) and the t_{Fout} is minimized using OP950 (1050 s). It should be highlighted that good results have been obtained also using the AP423, while ZB and OP950 show again the worst properties.

3.2.4. Samples with envelope and with FRs in the core

From Fig. 3d it is possible to observe that in case of samples with envelope but with the FR only in the core, the curves are characterized by two distinct peaks of the HRR, the first probably caused by the combustion of the envelope and the second due to the combustion of the EPDM matrix. With respect to the curves reported in Fig. 3b, it is immediately possible to notice the beneficial effect of the envelope: the curves are, indeed, characterized by lower HRR values and longer combustion times (both factors are indicating the lower violence of the combustion).

The efficacy of the envelope may be related to the presence of silica, talc and kaolin that probably interact with the FRs present in the core material: as observed by Dzulkafli et al. and Ullah et al. [51,53], talc and kaolin improve the intumescence of ammonium polyphosphate, the first due to the formation of a silicate layer that acts as a barrier protecting the underlying material and the second enhancing the char expansion with a consequent heat shielding of the substrate. On the other hand, silica can migrate from the ignition surface of the composites to the surface of carbon layer contributing to the efficacy of the intumescent layer [55]. Moreover, the charring activity of NBR rubber can further increase the benefits related to the presence of the envelope [73,74]: from the results reported in Table 3 it can be observed that, in case of ENV sample, the residual mass is around 58 wt% and, excluding the mineral fillers (around 33 wt%), the remaining part can be attributed to the combustion residue of NBR.

In addition, it can be observed that all the FRs lead to a decrease of HRR values. In particular, looking at the results reported in Table 3, it is possible to observe that the best results are obtained using the AP423: the HRR_{peak1} and HRR_{peak2} are decreased from 266 kW/m^2 and 318 kW/m^2 (in case of E+P+ENV) down to 225 kW/m^2 and 246 kW/m^2 by using the AP423. The MARHE is decreased from 239 kW/m^2 to 188 kW/m^2 by using the AP423. The t_{ign} is maximized using AP766 and OP950 (43 s) and the t_{Fout} is minimized using OP950 (1161 s). It can be hypothesised that the good results obtained using AP423 arise also from the positive interaction between clay and ammonium polyphosphate that allows the formation of a carbonaceous-silicate charred layer that protects the underlying material from excessive temperature increase [49]. The AP766 and OP950 leads to a value of MARHE higher with respect to AP423: it may be therefore hypothesised that the interactions between phosphinates (aluminium diethyl phosphinate in AP766 and zinc diethyl phosphinate in OP950) and the mineral fillers are less effective (or absent) with respect to those between APP and the interactions with the mineral fillers. Moreover, it can be concluded that mineral fillers will react mainly with APP and less with phosphinates. The absence of interactions between ZB and other elements present in the samples can be also hypothesised.

3.2.5. Samples with envelope and with FRs in the envelope

From Fig. 3e it is possible to observe that in case of samples with envelope and with the FR only in the envelope, the curves are characterized again by two distinct peaks of the HRR, the first probably caused by the combustion of the envelope (the presence of FR lead, indeed, to a decrease of the first peak) and the second due to the combustion of the EPDM matrix. With respect to the curves reported in Fig. 3d, it is possible to observe that in this case the curves present higher HRR values, meaning that the addition of FR is less effective in the envelope with respect to the core (this can be also observed comparing the MARHE values listed in Table 3). The positive effect of silica, kaolin and talc is probably present also in this case, but the absence of FRs in the core material probably results in the absence of other important interactions (such as between clay and APP). In this case is seems that ZB leads to better results with respect to the previous cases due to the formation of a glassy structure able to protect the underlying material: in particular the MARHE values obtained using ZB are lower with respect to the ones obtained using AP423. Indeed, looking at the results reported in Table 3, it is possible to observe that the best results are obtained using the AP766: the HRR_{peak1} and HRR_{peak2} are decreased from 266

kW/m^2 and 318 kW/m^2 (in case of E+P+ENV) down to 213 kW/m^2 and 250 kW/m^2, respectively. The MARHE is decreased from 239 kW/m^2 to 188 kW/m^2. The t_{ign} is maximized using AP766 (82 s) and the t_{Fout} is minimized using AP423 (1295 s).

3.2.6. Samples with envelope and with FRs in the core and in the envelope

From Fig. 3f it is possible to observe that in case of samples with envelope and with the FR both in the envelope and in the core, the curves are characterized by the lowest HRR values, with the sample containing

AP766 that shows the lowest values and the presence of a plateau instead of the second HRR peak, confirming the beneficial effect of the AP766 on the reduction of the combustion violence and combustion speed. Looking at the results reported in Table 3, it is possible to confirm the best performances of the AP766: the HRR_{peak1} and HRR_{peak2} are decreased from 266 kW/m^2 and 318 kW/m^2 (in case of E+P+ENV) down to 186 kW/m^2 and 209 kW/m^2, respectively. The maximum average rate of heat emission (MARHE) is significantly decreased upon addition of AP766 from 239 kW/m^2 to 175 kW/m^2. The use of AP423 as FR seems to be less effective with respect to AP766 but allows to obtain a longer ignition time (t_{ign}) that is increased from 42 s in case of E+P+ENV to 128. The better results obtained from the use of AP423 and AP766 with respect to other FRs may be the result of different interactions between ammonium polyphosphate, clay and talc, as previously stated. Moreover, the better results of AP766 are probably related to further interactions between ammonium polyphosphate, clay, talc,

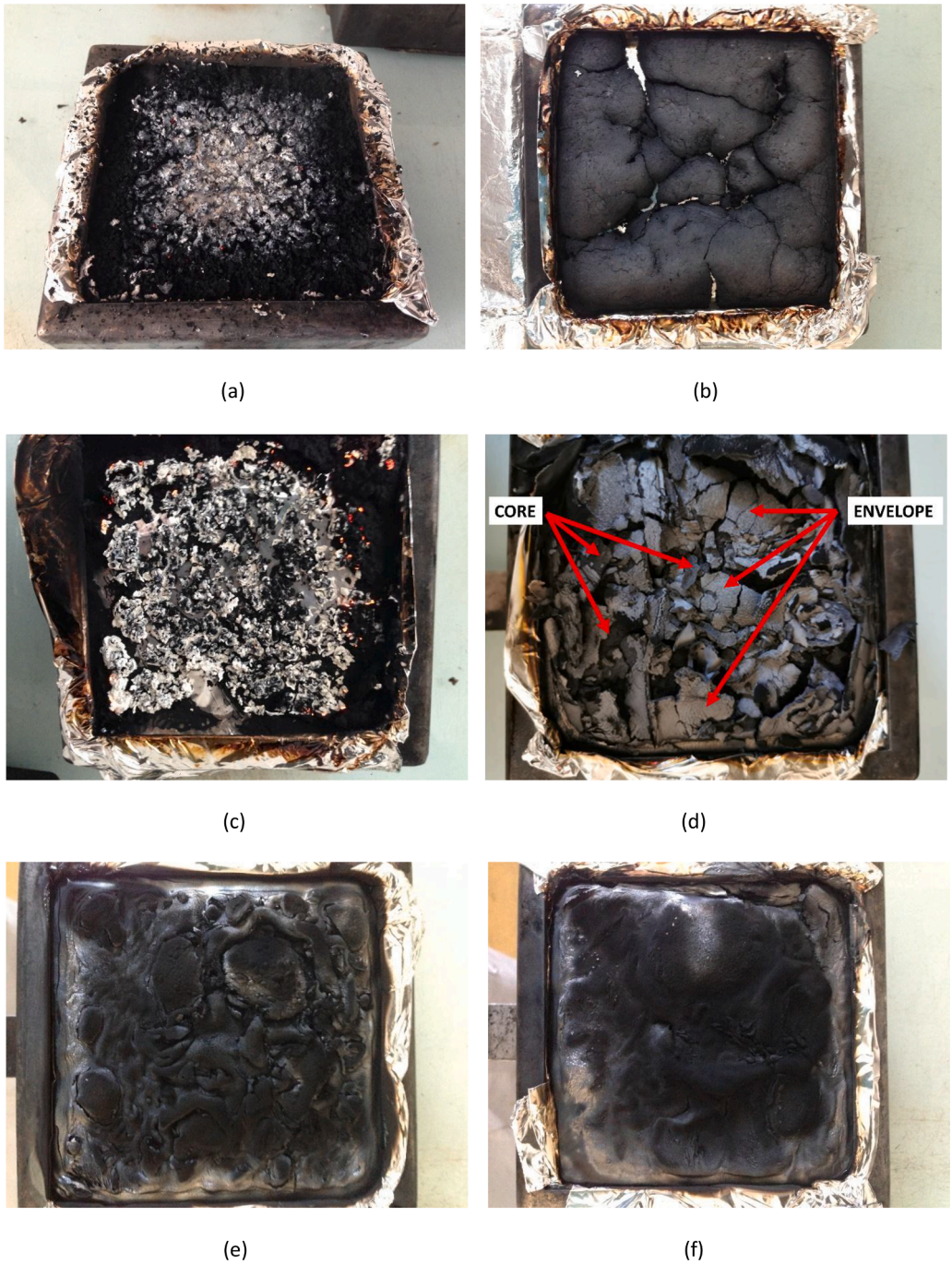

Fig. 4. Pictures of the combustion residues after cone calorimeter of selected samples: E (a), E+P (b), E+P_NC (c), E+P+ENV (d), E+P+766+ENV+766 (e), E+P+423+ENV+423 (f).

kaolin and aluminium diethyl phosphinate.

3.3. Combustion residues from cone calorimeter tests

Observing the pictures of the combustion residues shown in Fig. 4 (a-f) it is possible to appreciate some differences between the selected samples that may allow a better comprehension of their fire behaviour. The EPDM sample (Fig. 4a) and the E+P_NC sample (Fig. 4c) are characterized by a very low amount of residues, principally ashes, meaning that almost all the material was able to burn and that any barrier against flame propagation was formed during the combustion. On the contrary, E+P sample (Fig. 4b) is characterized by the presence of a higher amount of compact residues thanks to the presence of the clay (this is also confirmed by the m_{res} values reported in Table 4). Examining the combustion residues of the E+P+ENV sample (Figs. 4d and S1), it is possible to identify an external cohesive layer formed by the combustion of the envelope. The underlying material (not visible), formed by the combustion residues of the core, is characterized by high porosity and good adhesion with the residues of the envelope. In case of E+P+766+ENV+766 (Fig. 4e) and E+P+423+ENV+423 (Fig. 4f) samples it is possible to observe that the FR present in the envelope allows the formation of a cohesive intumescent layer acting as a barrier against flame propagation. Also in this case the combustion residues of the core (not visible) form a second intumescent structure, characterized by high porosity and good adhesion with the combustion residues of the envelope.

3.4. Evaluation of self-extinguishing ability with epiradiateur

Looking at the results of the epiradiateur tests listed in Table 4, it is possible to verify the effect of the flame retardants (FR) applied in different ways to the prepared samples and to compare the fire behaviour with respect to the reference samples without FR.

Table 4
Results of self-extinguishing ability tests.

Sample	t_{ign} [s]	$N_{ign\_5'}$ [-]	$t_{combustion\_tot}$ [s]
E	37 ± 3	3 ± 1	372 ± 162
E+P	11 ± 1	1 ± 0	723 ± 4
E+P_NC	12 ± 2	3 ± 2	358 ± 28
E+P+ENV	15 ± 6	4 ± 3	391 ± 140
E+P+ENV_NC	18 ± 2*	1 ± 1*	804 ± 82*
E+P+766	10 ± 1	1 ± 0	531 ± 42
E+P+423	13 ± 1	1 ± 0	526 ± 74
E+P+950	12 ± 1	1 ± 0	538 ± 25
E+P+ZB	11 ± 1	1 ± 0	611 ± 155
ENV	11 ± 1	1 ± 0	39 ± 14
ENV+766	11 ± 1	1 ± 0	40 ± 15
ENV+423	10 ± 1	1 ± 0	46 ± 6
ENV+950	10 ± 0	1 ± 0	51 ± 6
ENV+ZB	9 ± 1	1 ± 0	46 ± 11
E+P+766+ENV	19 ± 2	6 ± 0	308 ± 55
E+P+423+ENV	20 ± 0	5 ± 1	311 ± 4
E+P+950+ENV	18 ± 8	5 ± 1	297 ± 24
E+P+ZB+ENV	20 ± 1	6 ± 1	290 ± 4
E+P+ENV+766	21 ± 4	8 ± 2	346 ± 70
E+P+ENV+423	15 ± 0	2 ± 0	589 ± 8
E+P+ENV+950	26 ± 4	4 ± 0	308 ± 21
E+P+ENV+ZB	18 ± 8	7 ± 2	259 ± 8
E+P+766+ENV+766	18 ± 3	8 ± 1	288 ± 11
E+P+423+ENV+423	15 ± 1	7 ± 4	354 ± 50
E+P+950+ENV+950	19 ± 1	3 ± 1	338 ± 31
E+P+ZB+ENV+ZB	15 ± 1	4 ± 1	352 ± 5

*Standard deviation value calculated as the mean value between all the standard deviation values obtained for the same parameter. Experimental problems occurred during the tests did not allow to collect the data and due to the elevated number of samples it was not possible to repeat the test.

3.4.1. Reference samples

Regarding reference samples without FR it is possible to observe that EPDM is characterized by a long ignition time (37 s), 3 ignitions and a total combustion time of 372 s. The beneficial effect of clay can be observed only in presence of the external envelope: the E+P_NC+ENV sample is characterized by only one ignition that lasted until the complete combustion of the material; on the other hand, the E+P+ENV sample is characterized by 4 ignitions and by a rapid extinction of the flame. This behaviour also confirms the beneficial effect of the envelope, and in particular of the mineral fillers present in its composition in creating a protective layer able to avoid flame propagation and to promote flame extinction. Looking at the temperature profiles shown in Fig. 5a, it is possible to observe that the EPDM sample, despite a minimal self-extinguishing ability, is characterized by a very limited temperature increase. On the other hand, the addition of the PCM (E+P and E+P_NC samples) leads to a very rapid temperature increase, probably due to the absence of the external envelope that, as it is possible to observe looking at the temperature profile of E+P+ENV, is able to limit the temperature increase.

3.4.2. Samples without envelope and with FRs in the core

Samples without envelope are characterized only by 1 ignition, meaning that, without envelope, they are unable to extinguish nearby the flame. With respect to the E+P sample, the addition of flame retardants leads to shorter burning time ($t_{combustion\_tot}$), highlighting the self-extinguishing ability of the samples. Looking at the temperature profiles (Fig. 5b) it is possible to observe that the samples are characterized by a first temperature increase due to the flame propagation on the specimen's side exposed to the heat source, a second rapid temperature increase (at around 200 s) occurs as soon as the flame propagates on the other side of the specimen (where the temperature was measured) and reaches very high values (up to 650 °C). These results indirectly confirm the importance of the envelope (i.e. the charring activity of NBR rubber) and of the mineral fillers present in the formation of a protective layer on the samples' surface. The presence of the envelope is therefore essential not only to avoid paraffin leakage but also to improve the fire resistance of the panels.

3.4.3. Envelopes

Similarly, envelopes are characterized by a very rapid combustion that consumes completely the material during the first ignition. Due to the very low amount of material and the rapid combustion, the addition of FRs does not improve the behaviour of these samples. In this case it was not possible to monitor the surface temperature due to the too rapid combustion (around 10 s).

3.4.4. Samples with envelope and with FRs in the core

Samples with envelope but with the FR only in the core show, similarly to cone calorimeter tests, both the beneficial effects of the external envelope and of FRs. The best results are obtained using AP766 and ZB: with respect to the E+P+ENV sample, the ignition time is increased from 15 s to 19 s (AP766) and 20 s (AP423, ZB), the number of ignitions is increased from 4 to 6 (AP766, ZB) and the combustion time is decreased from 391 s to 290 s (ZB) and 308 s (AP766). Despite the absence of FR in the envelope, it is clear the beneficial effect of the mineral fillers (talc, kaolin and silica) and of the charring activity of NBR in creating a protecting layer able to increase the ignition time (almost doubled with respect to samples without ENV) and to increase the self-extinguishing ability of the samples (E+P+766+ENV is characterized by 6 ignitions, while E+P+766 only by 1). Looking at the temperature profiles (Fig. 5c) it is possible to observe that at the beginning the temperature is maintained at very low values thanks to the presence of the envelope that allow a rapid extinction of the flame. As soon as the envelope is damaged and the flame propagates, the temperature rises but is limited to values below 150 °C due to the limited intensity and extension of the flame.

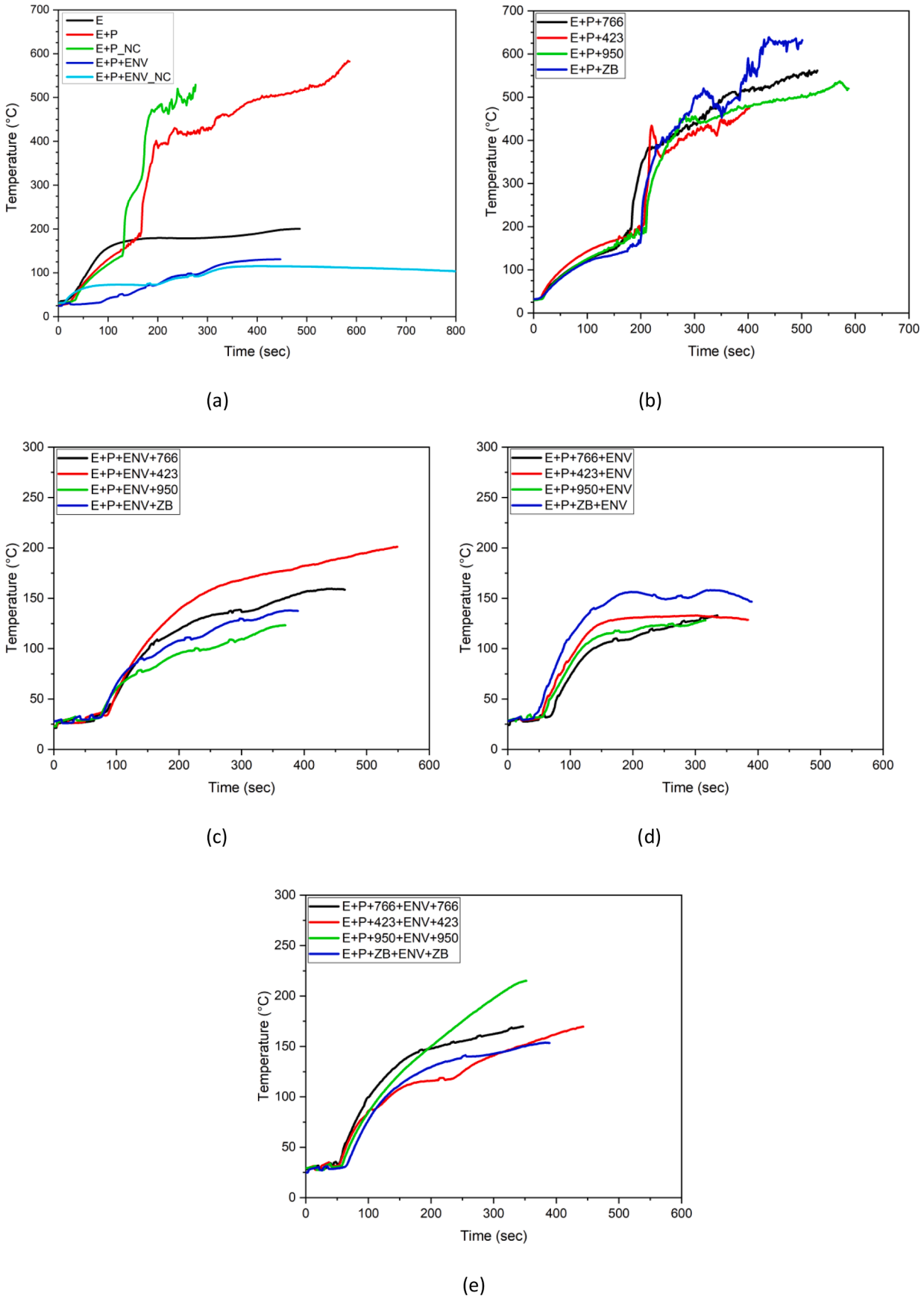

Fig. 5. Representative curves of surface temperature as function of time for the tested samples: reference samples (a), E+P+FR (b), E+P+ENV+FR (c), E+P+FR+ENV (d), E+P+FR+ENV+FR (e).

3.4.5. Samples with envelope and with FRs in the envelope

Samples with envelope and with the FR only in the envelope show, in some cases better results with respect to the previous case, worse in others. The ignition time is maximized in case of OP950 (26 s), the number of ignitions in case of AP766 (8 ignitions) and ZB (7 ignitions) and the combustion time is minimized in case of ZB (259 s). The AP423 lead to the worst results with an ignition time of 15 s, only 2 ignitions and a total combustion time of 589 s. It seems therefore that OP950 is very effective if applied in the envelope, while AP423 is more effective in the core; AP766 and ZB seem to be equally effective both in the core and in the envelope. The results obtained from the E+P+766+ENV sample may confirm the advantageous combination between mineral fillers and ammonium polyphosphate and between aluminium diethyl phosphinate and ammonium polyphosphate, already observed during the cone calorimeter tests. However, the good results obtained by using ZB should be underlined: despite its limited efficacy observed with cone calorimeter tests, it seems to be very effective in increasing the self-extinguishing ability of the samples thanks to the formation of a glassy structure (maybe incorporating the mineral fillers present in the envelope) able to avoid flame propagation.

Looking at the temperature profiles (Fig. 5d) it is possible to observe that the temperature plateau is longer with respect to the previous case thanks to the presence of the FRs that increases the ability of the samples to immediately extinguish the flame limiting the damage to the envelope. As soon as the envelope is damaged and the flame propagates, the temperature rises reaching higher values with respect to the previous case due to the absence of FRs in the core.

3.4.6. Samples with envelope and with FRs in the core and in the envelope

Similarly to cone calorimeter tests, samples with envelope and with the FR both in the envelope and in the core are characterized by the best performances but in this case it seems that the beneficial effect is mainly due to the envelope and to the presence of FR in the envelope that allows the formation of an intumescent layer able to extinguish the flame. The

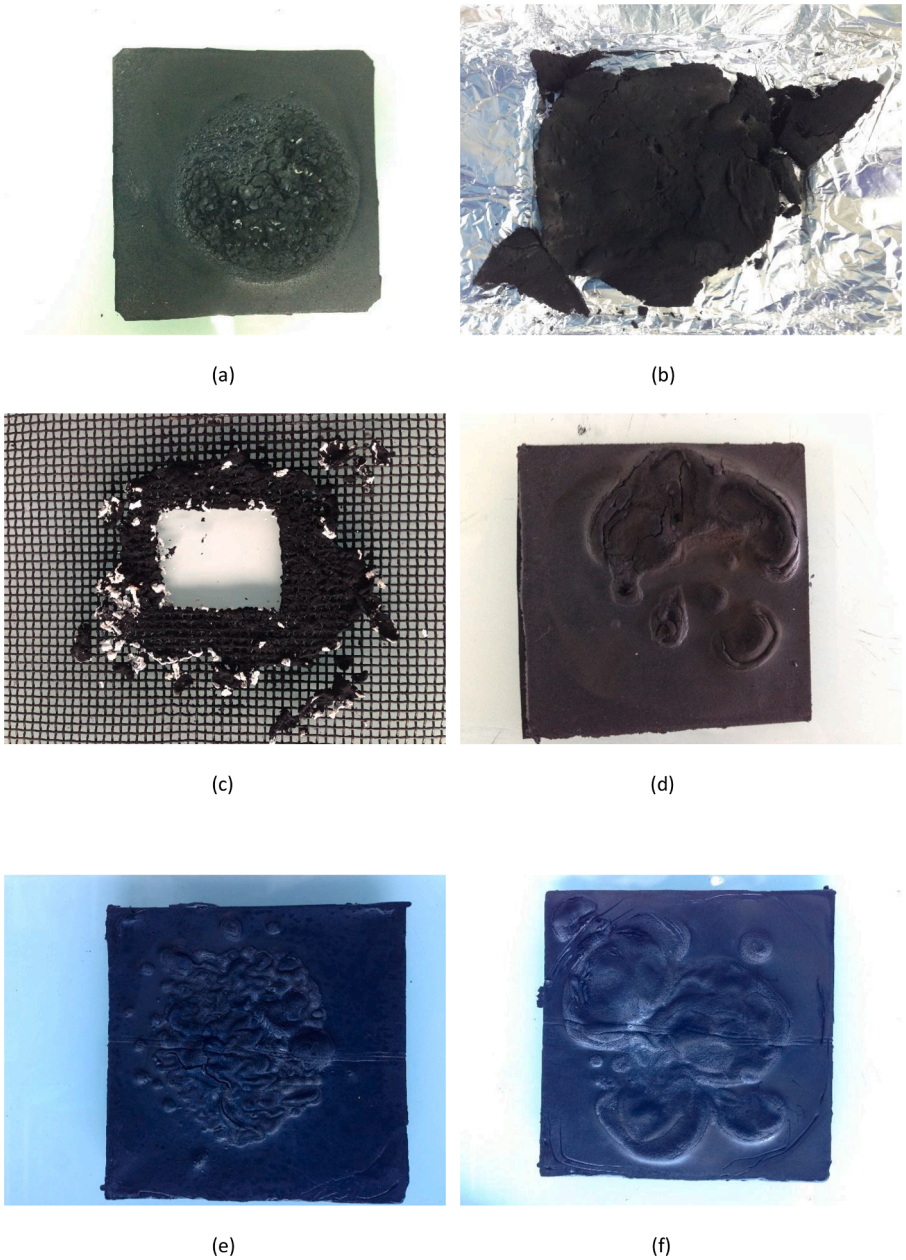

Fig. 6. Pictures of the combustion residues after epiradiateur test of selected samples: E (a), E+P (b), E+P_NC (c), E+P+ENV (d), E+P+766+ENV+766 (e), E+P+423+ENV+423 (f).

presence of FRs in the core seems to be effective only for the reduction of the total combustion time: the reason for this behaviour is that the envelope is very effective in promoting the flame extinguishing during the first ignitions and only when the prolonged and repeated combustion leads to its damage the presence of FR in the core become relevant. The best results are obtained in the case of AP766 that leads to an ignition time of 18 s, a number of ignitions equal to 8 and to a total combustion time of 288 s. The best results obtained from the AP766 with respect to the other FRs, although they show good properties if applied individually in the core or in the envelope, are probably related to the combination of all the interactions between ammonium polyphosphate and clay, talc, kaolin, silica and aluminium diethyl phosphinate that do not occur (or only partially occur) using other FR. Looking at the temperature profiles (Fig. 5e) it is possible to observe that the samples are characterized by temperature profiles slightly higher with respect to the E+P+ENV sample (Fig. 5a): this means that the FRs are useful to promote the self-extinguishing ability of the samples but do not have a beneficial effect in the decrease of their surface temperature during the combustion.

3.5. Combustion residues from epiradiateur tests

Observing the pictures of the combustion residues shown in Fig. 6(a-f) it is possible to appreciate some differences between the selected samples that may allow a better comprehension of their fire behaviour. The EPDM sample (Fig. 6a) is characterized by a very small combustion area, demonstration of its ability to avoid flame propagation. The E+P sample (Fig. 6b) is completely burned but the residues are compact thanks to the presence of the clay. The E+P-NC sample (Fig. 6c) is completely burned with a very limited amount of combustion residues. Comparing the E+P and the E+P+ENV samples (Fig. 6d), it is evident the beneficial effect of the envelope that, thanks to the charring activity of NBR and the presence of kaolin, talc and silica, is able to create a barrier against flame propagation and to promote the self-extinguishing ability of the material.

A similar behaviour occurs also in the E+P+766+ENV+766 sample (Fig. 6e), where it is possible to observe the formation of an intumescent layer of the surface that prevent the flame propagation to the core material. On the contrary, in the E+P+423+ENV+423 sample (Fig. 6f), the FR seems to have less efficacy in confining the flame propagation that, despite the presence of FR, is able to rapidly damage the external envelope.

3.6. Thermogravimetric analysis

Selected compositions based on the best FR (AP766) and inorganic fillers (silica, talc, kaolin in NBR and organomodified clay in EPDM) were tested by TGA analysis, in order to shed more light on thermodegradation of the tested compounds. Representative thermogravimetric curves are shown in Fig. 7 and the related results listed in Table 5.

The degradation of the reference sample (E+P+ENV) could be depicted by around 5 degradation steps, as evidenced by the DTGA curve: the first one at around 251 °C (T_{peak1}) due to the paraffin degradation (mass loss about 46 wt%), followed by a small shoulder at around 300 °C due to the decomposition reaction of alkyl ammonium salts present in the organomodified clay (see Fig. S2 and Table S4) [75]. The second peak at around 485 °C (T_{peak2}) is caused the degradation of the EPDM rubber and it is pre-empted by a shoulder at around 400 °C due to the degradation of the NBR rubber of the envelope [16]. In the range 518–598 °C two minor peaks can be identified. The first peak is caused by the dehydroxylation of kaolin [76] that occurs at around 518 °C, as can be observed in Fig. S2. Conversely, talc and silica are stable until 900 and 1000 °C, respectively [77,78]. The second peak can be associated to the decomposition of the carbonaceous fillers of the EPDM matrix [16].

The flame retardant AP766 is stable until 270 °C ($T_{5\%}$) and then its degradation occurs within three steps: the first at around 286 °C due to the release of NH_3, polyphosphoric acid and H_2O caused by the degradation of APP associated to a change of the crystalline form of APP into vitreous crosslinked ultraphosphate under the influence of heat [79–82], the second one at around 339 °C due to the partial vaporisation and partial decomposition of aluminium diethyl phosphinate to diethylphosphinic acid and ethane, with aluminium phosphates remained in the residue [79,80,83,84] and the third one at around 567 °C due to the transformation of the crosslinked vitreous ultraphosphate of APP into a volatile form of phosphorus oxide [79,80]. The sample E+P+766 is characterized by two main peaks at 253 °C (T_{peak1}) and 458 °C (T_{peak2}) related to the thermal degradation of paraffin (about 52 wt%) and EPDM rubber compound (about 23 wt%), respectively. The presence of AP766 can be detected observing a shoulder at 307 °C (T_{peak2}) and a small peak at around 590 °C (T_{peak3}). The evident shoulder at around 300 °C is caused by the decomposition of ammonium salts present in the organomodified clay (see Fig. S2). Moreover, the residue of about 19 wt% at 700 °C derived from both AP766 and organomodified clay (the residue

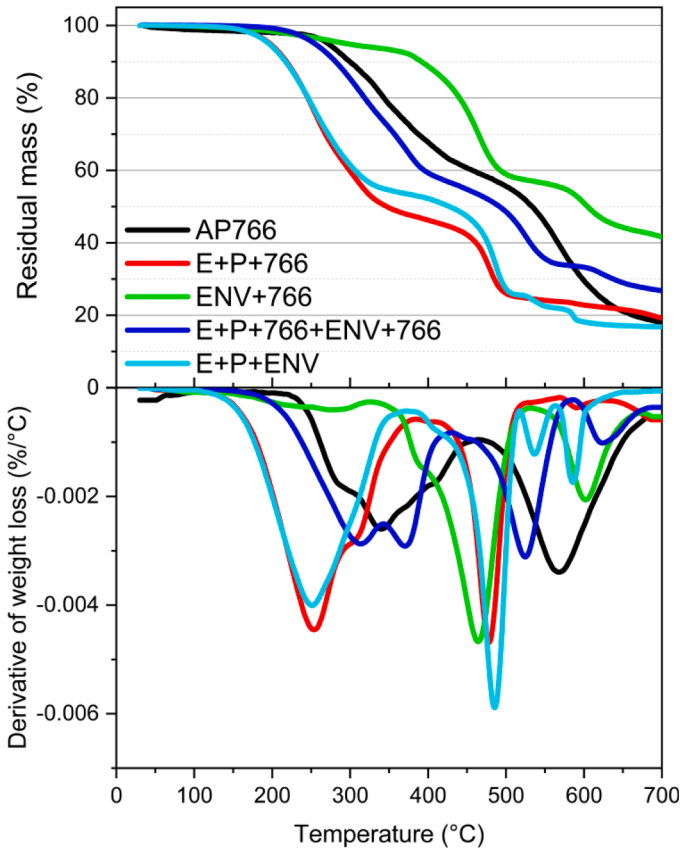

Fig. 7. Thermogravimetric analysis curves of selected samples: AP766, E+P+ENV, E+P+766, ENV+766, E+P+766+ENV+766.

Table 5
Results of TGA tests.

Sample	$T_{5\%}$ [°C]	T_{peak1} [°C]	T_{peak2} [°C]	T_{peak3} [°C]	m_{700} [wt %]
AP766	272	339.0	567.3	-	18.0
E+P+766	197	253.7/ 307.5	478.2	-	19.2
ENV+766	295	-	464.2	602.5	41.8
E+P+766+ENV+766	254	312.8/ 370.5	524.5	623.5	26.8
E+P+ENV (ref)	196	251.5	485.5	536.8/ 585.5	16.9

of pristine organomodified clay is about 63 wt%, as documented in Table S4).

The envelope (ENV+766) is characterized by a minor degradation step at around 200 °C caused by the mass loss of oils and low molecular weight plasticizer, and by two main degradation steps at 464 °C and 602 °C due to the degradation of the elastomer and to the dehydroxilation of kaolin, respectively. Moreover, as observed by Batistella et al., interactions between kaolinite and the phopshinates present in the AP766 can occur in the same temperature range [85]. The presence of the AP766 can be detected by a small shoulder at around 380 °C.

Finally, the E+P+766+ENV+766 sample shows a very complex degradation curve, as combined results derived from the sum of each component in the formulation. It is interesting to notice that the paraffin degradation is shifted to higher temperature of more than 60 °C (316 °C). The other degradation steps can be attributed to the degradation of the aluminium diethyl phosphinate (at 371 °C), the degradation of the elastomeric NBR components (at 574 °C) slightly higher than that of pristine without flame retardant AP766 [16] and the decomposition of the carbonaceous fillers and volatilization of phosphorus oxide (at 623 °C).

The flame retardant AP766 is characterized by a residual mass (m_{700}) of around 18 wt% due to the formation of intumescent material. The residual mass value is the highest for ENV+766 sample (41.8 wt%) due the high amount of mineral fillers (33 wt%), the presence of residual flame retardant (around 3 wt% of the residual mass) and the residues from the degradation of the elastomeric compound (around 5–6 wt% of the residual mass). The residual mass of E+P+766+ENV+766 is around 27 wt% and this value is the sum of the residues of the core material, of the envelope and of the flame retardant (E+P+766 about 19 wt%; ENV+766 about 42 wt%). It is interesting to notice, as also observed in Table S4, the charring ability of NBR rubber (and minorly of EPDM) evidenced by the high value of residual mass.

The positive effect of AP766 with inorganic or organic additives in thermal degradation and its role as flame retardant has been also confirmed and described in literature [86–89].

4. Conclusions

In this work the fire behaviour of EPDM/NBR panels containing paraffin for thermal energy storage applications and four different flame retardants was deeply investigated. FRs were added selectively only in the core material, only in the envelope and both in the core and envelope in order to verify their efficacy. From cone calorimeter tests it was observed the positive effect of clay related to the formation of a carbonaceous-silicate charred layer and to the positive interaction with ammonium polyphosphate. The results reported a strong decrease of HRR_{peak2} from 618 kW/m^2 in case of E+P_NC (sample without clay) to 467 kW/m^2 in case of E+P (sample with clay). Moreover, also the beneficial role of the envelope was observed: the charring activity of NBR rubber and the presence of mineral fillers (talc, kaolin and silica) led to the formation of a protective layer, acting as a barrier able to reduce the fire intensity and to promote the extinction of the flame. The results showed a decrease from 467 to 318 kW/m^2 of the peak of HRR and from 383 to 239 kW/m^2 of the MARHE in case of samples without and with envelope, respectively. Positive interactions between ammonium polyphosphate and the mineral fillers, able to improve intumescence phenomena, were also observed. A decrease from 318 to 246 kW/m^2 of the peak of HRR and from 239 to 188 kW/m^2 of the MARHE was observed in case of samples E+P+ENV and E+P+423+ENV, respectively. In addition, it was possible to identify the FR with the best performances (Clariant Exolit® AP766) probably related not only to the advantageous combination between ammonium polyphosphate and the mineral fillers (clay, talc, kaolin and silica) that led to the formation of a protective layer with barrier effect, but also to those between ammonium polyphosphate and aluminium diethyl phosphinate. The best performances were obtained by adding FRs both in the core and in the envelope material: it was possible to decrease the peak of the heat release rate (HRR) from 318 kW/m^2 to 209 kW/m^2 and the MARHE (parameter describing the intensity of the combustion over the whole process of thermal degradation) from 239 kW/m^2 to 175 kW/m^2. From tests to evaluate the self-extinguishing ability of the prepared samples it was possible to observe the extreme importance of the envelope in improving the self-extinguishing ability of the samples: this confirmed the importance of NBR rubber composition able to promote charring activity (here superior than that of EPDM one without FR) and particularly the beneficial effect of the mineral fillers (talc, kaolin and silica) and their interactions with ammonium polyphosphate. Moreover, it was also evidenced the beneficial effect of clay and the best performances of Clariant Exolit® AP766 were also confirmed. The best composition allowed to increase the ignition time from 15 to 18 s, to increase the number of ignitions within 5 min, from 4 to 8 and to decrease the total combustion time from 391 to 288 s. In conclusion, it was possible to improve the fire behaviour of EPDM/NBR samples with paraffin in order to make possible future applications in the field of thermal energy storage of buildings. From the economical point of view, it is possible to evaluate a cost increase of only 3% for the E+P+766+ENV+766 sample with respect to the E+P+ENV and an enthalpy reduction of 23% that seems reasonable considering the advantage given from the increased safety of the material in terms of fire resistance. The second part of this work [63] is devoted to a detailed investigation of the combustion residues using Nuclear Magnetic Resonance, Energy-Dispersive X-Ray Spectroscopy and X-Ray Diffraction in order to understand the mechanisms behind the flame retardancy of Clariant Exolit® AP766.

CRediT authorship contribution statement

Francesco Valentini: Conceptualization, Data curation, Formal analysis, Investigation, Methodology, Validation, Visualization, Writing – original draft. **Jean-Claude Roux:** Investigation, Methodology, Validation. **Josè-Marie Lopez-Cuesta:** Conceptualization, Formal analysis, Methodology, Validation, Writing – review & editing. **Luca Fambri:** Methodology, Validation, Supervision, Writing – review & editing. **Andrea Dorigato:** Supervision, Writing – review & editing. **Alessandro Pegoretti:** Methodology, Supervision, Funding acquisition, Writing – review & editing.

Declaration of Competing Interest

The authors declare that they have no known competing financial interests or personal relationships that could have appeared to influence the work reported in this paper

Acknowledgements

This work was partially funded by Provincia Autonoma di Trento (Italy) through Legge 6/99, project “Compositi elastomerici a transizione di fase [E-PCM] prat. n. 23-16”.

Supplementary materials

Supplementary material associated with this article can be found, in the online version, at doi:10.1016/j.polymdegradstab.2022.110240.

References

[1] A. GhaffarianHoseini, N.D. Dahlan, U. Berardi, A. GhaffarianHoseini, N. Makaremi, M. GhaffarianHoseini, Sustainable energy performances of green buildings: a review of current theories, implementations and challenges, Renew. Sustain. Energy Rev. 25 (2013) 1–17.
[2] A. Haque, Solar energy, Electr. Renew. Energy Syst. (2016) 40–59.
[3] J.W. Tester, E.M. Drake, M.J. Driscoll, M.W. Golay, W.A. Peters, Sustainable Energy: Choosing Among Options, Massachussets Institute of Technology, 2012.

[4] N. Belyakov. Sustainable Power Generation: Current Status, Future Challenges, and Perspectives, Academic Press, 2019, pp. 417–438, https://doi.org/10.1016/B978-0-12-817012-0.00031-1.

[5] P. Meshgin, Y.P. Xi, Y. Li, Utilization of phase change materials and rubber particles to improve thermal and mechanical properties of mortar, Constr. Build. Mater. 28 (1) (2012) 713–721.

[6] B. He, V. Martin, F. Setterwall, Phase transition temperature ranges and storage density of paraffin wax phase change materials, Energy 29 (11) (2004) 1785–1804.

[7] M.R. Anisur, M.H. Mahfuz, M.A. Kibria, R. Saidur, I.H.S.C. Metselaar, T.M. I. Mahlia, Curbing global warming with phase change materials for energy storage, Renew. Sustain. Energy Rev. 18 (2013) 23–30.

[8] D. Fernandes, F. Pitié, G. Cáceres, J. Baeyens, Thermal energy storage: "How previous findings determine current research priorities, Energy 39 (1) (2012) 246–257.

[9] H. Bo, E.M. Gustafsson, F. Setterwall, Phase transition temperature ranges and storage density of paraffin wax phase change materials, Energy 24 (12) (1999) 1015–1028.

[10] S. Peng, A. Fuchs, R.A. Wirtz, Polymeric phase change composites for thermal energy storage, J. Appl. Polym. Sci. 93 (2004) 1240–1251.

[11] A.M. Borreguero, M. Carmona, M.L. Sanchez, J.L. Valverde, J.F. Rodriguez, Improvement of the thermal behaviour of gypsum blocks by the incorporation of microcapsules containing PCMS obtained by suspension polymerization with an optimal core/coating mass ratio, Appl. Thermal Eng. 30 (10) (2010) 1164–1169.

[12] A. Dorigato, M.V. Ciampolillo, A. Cataldi, M. Bersani, A. Pegoretti, Polyethylene wax/EPDM blends as shape-stabilized phase change materials for thermal energy storage, Rubber Chem. Technol. 90 (3) (2017) 575–584.

[13] X. Kong, C. Yao, P. Jie, Y. Liu, C. Qi, X. Rong, Development and thermal performance of an expanded perlite-based phase change material wallboard for passive cooling in building, Energy Build. 152 (2017) 547–557.

[14] C. Yao, X. Kong, Y. Li, Y. Du, C. Qi, Numerical and experimental research of cold storage for a novel expanded perlite-based shape-stabilized phase change material wallboard used in building, Energy Convers. Manag. 155 (2018) 20–31.

[15] L.F. Cabeza, C. Castellón, M. Nogués, M. Medrano, R. Leppers, O. Zubillaga, Use of microencapsulated PCM in concrete walls for energy savings, Energy Build. 39 (2) (2007) 113–119.

[16] F. Valentini, A. Dorigato, L. Fambri, M. Bersani, M. Grigiante, A. Pegoretti, Production and characterization of novel EPDM/NBR panels with paraffin for potential thermal energy storage applications, Thermal Sci. Eng. Progr. 32 (2022) 101309.

[17] G. Song, S. Ma, G. Tang, Z. Yin, X. Wang, Preparation and characterization of flame retardant form-stable phase change materials composed by EPDM, paraffin and nano magnesium hydroxide, Energy 35 (2015) 2179–2183.

[18] C. Alkan, K. Kaya, A. Sari, Preparation, thermal properties and thermal reliability of form-stable paraffin/polypropylene composite for thermal energy storage | springerlink, J. Polym. Environ. 17 (2009) 254.

[19] W.-I. Cheng, R.-m. Zhang, K. Xie, N. Liu, J. Wang, Heat conduction enhanced shape-stabilized paraffin/HDPE composite PCMs by graphite addition: preparation and thermal properties, Sol. Energy Mater. Sol. Cells 94 (10) (2010) 1636–1642.

[20] H. Inaba, P. Tu, Evaluation of thermophysical characteristics on shape-stabilized paraffin as a solid-liquid phase change material, Heat Mass Transfer 32 (4) (2019) 307–312.

[21] K. Kaygusuz, A. Sari, High density polyethylene/paraffin composites as form-stable phase change material for thermal energy storage, Energy Sources, Part A: Recov., Utiliz. Environ. Effects 29 (3) (2007) 261–270.

[22] K. Kaygusuz, C. Alkan, A. Sari, O. Uzun, Encapsulated fatty acids in an acrylic resin as shape-stabilized phase change materials for latent heat thermal energy storage, Energy Sources, Part A: Recov., Utiliz. Environ. Effects 30 (2008).

[23] W. Mhike, W.W. Focke, J.P.L. Mofokeng, Thermally conductive phase-change materials for energy storage based on low-density polyethylene, soft Fischer–Tropsch wax and graphite, Thermochim. Acta 572 (2012) 75–82.

[24] M. Xiao, B. Feng, K. Gong, Preparation and performance of shape stabilized phase change thermal storage materials with high thermal conductivity, Energy Convers. Manag. 43 (1) (2002) 103–108.

[25] Y. Hong, G. Xin-shi, Preparation of polyethylene–paraffin compound as a form-stable solid-liquid phase change material, Sol. Energy Mater. Sol. Cells 64 (1) (2000) 37–44.

[26] I. Krupa, G. Mikova, A.S. Luyt, Polypropylene as a potential matrix for the creation of shape stabilized phase change materials, Eur. Polym. J. 43 (3) (2007) 895–907.

[27] A. Sari, C. Alkan, A. Karaipekli, O. Uzun, Poly(ethylene glycol)/poly(methyl methacrylate) blends as novel form-stable phase-change materials for thermal energy storage, J. Appl. Polym. Sci. 116 (2) (2009) 929–933.

[28] Q. Cao, L. Pengsheng, Hyperbranched polyurethane as novel solid–solid phase change material for thermal energy storage, Eur. Polym. J. 42 (11) (2006) 2931–2939.

[29] F. Valentini, A. Dorigato, A. Pegoretti, M. Tomasi, G.D. Sorarù, M. Biesuz, Si3N4 nanofelts/paraffin composites as novel thermal energy storage architecture, J. Mater. Sci. 56 (2) (2020) 1537–1550.

[30] A. Petsom, S. Roengsumran, A. Ariyaphattanakul, P. Sangvanich, An oxygen index evaluation of flammability for zinc hydroxystannate and zinc stannate as synergistic flame retardants for acrylonitrile–butadiene–styrene copolymer, Polym. Degrad. Stab. 80 (1) (2003) 17–22.

[31] P. Sittisart, M.M. Farid, Fire retardants for phase change materials, Appl. Energy 88 (9) (2011) 3140–3145.

[32] Y. Cai, Y. Hu, L. Song, Y. Tang, R. Yang, Y. Zhang, Z. Chen, W. Fan, Flammability and thermal properties of high density polyethylene/paraffin hybrid as a form-stable phase change material, J. Appl. Polym. Sci. 99 (4) (2006) 1320–1327.

[33] European Commission, Commission Regulation (EU) 2019/2021 of 1 *October 2019 laying down ecodesign requirements for electronic displays pursuant to Directive 2009/125/EC of the European Parliament and of the Council, amending Commission Regulation (EC) No 1275/2008 and repealing Commission Regulation (EC) No 642/2009 (Text with EEA relevance.)*. 2019.

[34] Sittisart, P. and M.M. Farid, Fire retardant for phase change material, in flame retardants. 2015. p. 187-207.

[35] H. Fiedler. Short-chain chlorinated paraffins: production, use and international regulations, Chlorinated Paraffins, Springer, Berlin, Heidelberg, 2010, pp. 1–40.

[36] M. Sharkey, S. Harrad, M. Abou-Elwafa Abdallah, D.S. Drage, H. Berresheim, Phasing-out of legacy brominated flame retardants: the UNEP Stockholm Convention and other legislative action worldwide, Environ. Int. 144 (2020), 106041.

[37] R. Kozlowski, D. Wesolek, M. Wladyka-Przybylak, S. Duquesne, A. Vannier, S. Bourbigot, R. Delobel, Intumescent flame-retardant treatments for flexible barriers. Multifunctional Barriers for Flexible Structure. Materials Science, Springer, Berlin, Heidelberg: Berlin, 2007.

[38] Y. Cai, Y. Hu, L. Song, Q. Kong, R. Yang, Y. Zhang, Z. Chen, W. Fan, Preparation and flammability of high density polyethylene/paraffin/organophilic montmorillonite hybrids as a form stable phase change material, Energy Convers. Manag. 48 (2) (2007) 462–469.

[39] F. Dabrowski, M.Le Bras, L. Cartier, S. Bourbigot, The use of clay in an EVA-based intumescent formulation. Comparison with the intumescent formulation using polyamide-6 clay nanocomposite as carbonisation agent, J. Fire Sci. 19 (3) (2016) 219–241.

[40] S.-H. Chiu, W.-K. Wang, Dynamic flame retardancy of polypropylene filled with ammonium polyphosphate, pentaerythritol and melamine additives, Polymer 39 (10) (1998) 1951–1955.

[41] Y. Tang, Y. Hu, S. Wang, Z. Gui, Z. Chen, W. Fan, Intumescent flame retardant-montmorillonite synergism in polypropylene-layered silicate nanocomposites, Polym. Int. 52 (8) (2003) 1396–1400.

[42] B. Tourea, J.-M. Lopez Cuesta, P. Gaudon, A. Benhassaine, A. Crespy, Fire resistance and mechanical properties of a huntite/hydromagnesite/antimony trioxide/decabromodiphenyl oxide filled PP-PE copolymer, Polym. Degrad. Stab. 56 (3) (1996) 371–379.

[43] L. Haurie, A.I. Fernández, J.I. Velasco, J.M. Chimenos, J.-M. Lopez Cuesta, F. Espiell, Thermal stability and flame retardancy of LDPE/EVA blends filled with synthetic hydromagnesite/aluminium hydroxide/montmorillonite and magnesium hydroxide/aluminium hydroxide/montmorillonite mixtures, Polym. Degrad. Stab. 92 (6) (2007) 1082–1087.

[44] F. Laoutid, P. Gaudon, J.M. Taulemesse, J.M. Lopez Cuesta, J.I. Velasco, A. Piechaczyk, Study of hydromagnesite and magnesium hydroxide based fire retardant systems for ethylene–vinyl acetate containing organo-modified montmorillonite, Polym. Degrad. Stab. 91 (12) (2006) 3074–3082.

[45] L. Clerc, L. Ferry, E. Leroy, J.-M. Lopez-Cuesta, Influence of talc physical properties on the fire retarding behaviour of (ethylene–vinyl acetate copolymer/magnesium hydroxide/talc) composites, Polym. Degrad. Stab. 88 (3) (2005) 504–511.

[46] Y.B. Cai, Q.F. Wei, D.F. Shao, Y. Hu, L. Song, W.D. Gao, Magnesium hydroxide and microencapsulated red phosphorus synergistic flame retardant form stable phase change materials based on HDPE/EVA/OMT nanocomposites/paraffin compounds, J. Energy Inst. 82 (1) (2009) 28–36.

[47] Y. Cai, Y. Hu, L. Song, H. Lu, Z. Chen, W. Fan, Preparation and characterizations of HDPE–EVA alloy/OMT nanocomposites/paraffin compounds as a shape stabilized phase change thermal energy storage material, Thermochim. Acta 451 (1-2) (2006) 44–51.

[48] Y.P. Khanna, E.M. Pearce, Synergism and flame retardancy, Flame - Retardant Polymeric Materials (1978) 43–61. M. Lewin, Editor.

[49] M. Zanetti, T. Kashiwagi, L. Falqui, G. Camino, Cone calorimeter combustion and gasification studies of polymer layered silicate nanocomposites, Chem. Mater. 14 (2) (2002) 881–887.

[50] X. Almeras, M.Le Bras, P. Hornsby, S. Bourbigot, G. Marosi, S. Keszei, F. Poutch, Effect of fillers on the fire retardancy of intumescent polypropylene compounds, Polym. Degrad. Stab. 82 (2) (2003) 325–331.

[51] H.H. Dzulkafli, F. Ahmad, S. Ullah, P. Hussain, O. Mamat, P.S.M. Megat-Yusoff, Effects of talc on fire retarding, thermal degradation and water resistance of intumescent coating, Appl. Clay Sci. 146 (2017) 350–361.

[52] T. Thuechart, W. Keawwattana, The effect of kaolin clay on fire retardancy and thermal degradation of intumescent flame retardant (IFR)/natural rubber composite, Adv. Mater. Res. 844 (2013) 334–337.

[53] S. Ullah, F. Ahmad, A.M. Shariff, M.A. Bustam, Synergistic effects of kaolin clay on intumescent fire retardant coating composition for fire protection of structural steel substrate, Polym. Degrad. Stab. 110 (2014) 91–103.

[54] G. Fang, H. Li, Z. Chen, X. Liu, Preparation and characterization of flame retardant n-hexadecane/silicon dioxide composites as thermal energy storage materials, J. Hazard. Mater. 181 (1-3) (2010) 1004–1009.

[55] Z.-H. Wu, J.-P. Qu, Y.-Q. Zhao, H.-L. Tang, J.-S. Wen, Flammable and mechanical effects of silica on intumescent flame retardant/ethylene–octene copolymer/polypropylene composites, J. Thermoplastic Compos. Mater. 28 (7) (2013) 981–994.

[56] Y. Yang, X. Shi, R. Zhao, Flame retardancy behavior of zinc borate, J. Fire Sci. 7 (1999) 355–361.

[57] C. Chen, Y. Zhou, W. He, C. Gao, X. Chen, J. Guo, M. Wang, Flammability, thermal stability, and mechanical propertiesof ethylene-propylene-diene monomer/polypropylenecomposites filled with intumescent flame retardant andinorganic synergists, J. Appl. Polym. Sci. 138 (2021) 1–14.

[58] Y. Hu, X. Wang, Flame Retardant Polymeric Materials: a Handbook, CRC Press Taylor & Francis Group, LLC, 2020.
[59] P. Hough, N. van der Aar, Z. Qiu, Compounding and mixing methodology for good performance of EPDM in tire sidewalls, Tire Sci. Technol. 48 (1) (2020) 2–21.
[60] A. Nasiri, N. Gontard, E. Gastaldi, S. Peyron, Contribution of nanoclay to the additive partitioning in polymers, Appl. Clay Sci. 146 (2017) 27–34.
[61] J.E. Jablonski, L. Yu, S. Malik, A. Sharma, A. Bajaj, S.L. Balasubramaniam, R. Bleher, R.G. Weiner, T.V. Duncan, Migration of quaternary ammonium cations from exfoliated clay/low-density polyethylene nanocomposites into food simulants, ACS Omega 4 (8) (2019) 13349–13359.
[62] A.A. Mousa, Y.A. Youssef, W.S. Mohamed, R. Farouk, E. Giebel, M.R. Buchmeiser, Organoclays assisted vat and disperse dyeing of poly(ethylene terephthalate) nanocomposite fabrics via melt spinning, Colorat. Technol. 134 (2) (2017) 126–134.
[63] Valentini, F., E. Callone, S. Dirè, J.-C. Roux, J.M. Lopez-Cuesta, G. Le Saout, L. Fambri, A. Dorigato, and A. Pegoretti, *Fire behaviour of EPDM/NBR panels with paraffin for thermal energy storage applications. Part 2: analysis of combustion residues.* Submitted.
[64] Ribeiro de Souza, D.A., Private communication.
[65] Technical Data Sheet of Exolit® AP766. Visited on 04/07/2022; Available from: https://www.clariant.com/en/Solutions/Products/2014/03/18/16/31/Exolit-AP-766?p=1.
[66] Technical Data Sheet of Exolit® AP423. Visited on 04/07/2022; Available from: https://www.clariant.com/en/Solutions/Products/2014/03/18/16/31/Exolit-AP-423?p=1.
[67] Technical Data Sheet of Exolit®OP950. Visited on 04/07/2022; Available from: https://www.clariant.com/en/Solutions/Products/2014/03/18/16/31/Exolit-OP-950?p=1.
[68] Technical Data Sheet of Firebrake® ZB. Visited on 04/07/2022; Available from: https://www.borax.com/BoraxCorp/media/Borax-Main/Resources/Data-Sheets/firebrake-zb.pdf?ext=.pdf.
[69] N. Didane, S. Giraud, E. Devaux, Fire performances comparison of back coating and melt spinning approaches for PET covering textiles, Polym. Degrad. Stab. 97 (7) (2012) 1083–1089.
[70] F. Valentini, L. Fambri, A. Dorigato, A. Pegoretti, Production and characterization of TES-EPDM foams with paraffin for thermal management applications, Front. Mater. 8 (2021) 101.
[71] M. Batistella, B. Otazaghine, R. Sonnier, C. Petter, J.-M. Lopez-Cuesta, Fire retardancy of polypropylene/kaolinite composites, Polym. Degrad. Stab. 129 (2016) 260–267.
[72] K.-S. Jang, Mineral filler effect on the mechanics and flame retardancy of polycarbonate composites: talc and kaolin, e-Polymers 16 (5) (2016) 379–386.
[73] Srivastava, S.K. and T. Kuila, Fire retardancy of elastomers and elastomer nanocomposites, in Polymer Green Flame Retardants. 2014. p. 597-651.Elsevier.
[74] M. Natali, M. Rallini, J. Kenny, L. Torre, Effect of Wollastonite on the ablation resistance of EPDM based elastomeric heat shielding materials for solid rocket motors, Polym. Degrad. Stab. 130 (2016) 47–57.
[75] J.M. Cervantes-Uc, J.V. Cauich-Rodríguez, H. Vázquez-Torres, L.F. Garfias-Mesías, D.R. Paul, Thermal degradation of commercially available organoclays studied by TGA–FTIR, Thermochim. Acta 457 (1) (2007) 92–102.
[76] Trusilewicz, L., F. Fernández-Martínez, V. Rahhal, and R. Talero, TEM and SAED characterization of metakaolin. pozzolanic activity. J. Am. Ceram. Soc., 2012. 95 (9): p. 2989-2996.
[77] V. Balek, J. Subrt, L.A. Pérez-Maqueda, M. Benes, I.M. Bountseva, I.N. Beckman, J. L. Pérez-Rodríguez, Thermal behavior of ground talc mineral, J. Min. Metall., Sect. B: Metall. 44 (1) (2008) 7–17.
[78] L. Klapiszewski, T.J. Szalaty, J. Zdarta, T. Jesionowski, Activated lignin and aminosilane-grafted silica as precursors in hybrid material production, Physicochem. Probl. Min. Process. 52 (1) (2016) 459–478.
[79] A. Riva, G. Camino, L. Fomperie, P. Amigouët, Fire retardant mechanism in intumescent ethylene vinyl acetate compositions, Polym. Degrad. Stab. 82 (2) (2003) 341–346.
[80] V. Realinho, L. Haurie, J. Formosa, J.I. Velasco, Flame retardancy effect of combined ammonium polyphosphate and aluminium diethyl phosphinate in acrylonitrile-butadiene-styrene, Polym. Degrad. Stab. 155 (2018) 208–219.
[81] G. Camino, L. Costa, L. Trossarelli, Study of the mechanism of intumescence in fire retardant polymers: part V—Mechanism of formation of gaseous products in the thermal degradation of ammonium polyphosphate, Polym. Degrad. Stab. 12 (3) (1985) 203–211.
[82] Z. Wang, E. Han, W. Ke, Influence of nano-LDHs on char formation and fire-resistant properties of flame-retardant coating, Progr. Org. Coat. 53 (1) (2005) 29–37.
[83] U. Braun, B. Schartel, M.A. Fichera, C. Jäger, Flame retardancy mechanisms of aluminium phosphinate in combination with melamine polyphosphate and zinc borate in glass-fibre reinforced polyamide 6,6, Polym. Degrad. Stab. 92 (8) (2007) 1528–1545.
[84] T. Orhan, N.A. Isitman, J. Hacaloglu, C. Kaynak, Thermal degradation mechanisms of aluminium phosphinate, melamine polyphosphate and zinc borate in poly (methyl methacrylate), Polym. Degrad. Stab. 96 (10) (2011) 1780–1787.
[85] M.A. Batistella, R. Sonnier, B. Otazaghine, C.O. Petter, J.M. Lopez-Cuesta, Interactions between kaolinite and phosphinate-based flame retardant in Polyamide 6, Appl. Clay Sci. 157 (2018) 248–256.
[86] D. Jung, I. Persi, D. Bhattacharyya, Synergistic effects of feather fibers and phosphorus compound on chemically modified chicken feather/polypropylene composites, ACS Sustain. Chem. Eng. 7 (23) (2019) 19072–19080.
[87] L. Floch, B. Da Cruz Chiochetta, L. Ferry, D. Perrin, P. Ienny, Fire protective surface coating containing nanoparticles for marine composite laminates, J. Compos. Sci. 5 (1) (2020) 6.
[88] C. Yargici Kovanci, M. Nofar, A. Ghanbari, Synergistic enhancement of flame retardancy behavior of glass-fiber reinforced polylactide composites through using phosphorus-based flame retardants and chain modifiers, Polymers (Basel) 14 (23) (2022) 5324.
[89] B. Zirnstein, D. Schulze, B. Schartel, Mechanical and fire properties of multicomponent flame retardant EPDM rubbers using aluminum trihydroxide, ammonium polyphosphate, and polyaniline, Materials (Basel) 12 (12) (2019) 1932.